Adsorption and Pattern Recognition of Polymers at Complex Surfaces with Attractive Stripelike Motifs

Monika Möddel[*] and Wolfhard Janke[†]

*Institut für Theoretische Physik and Centre for Theoretical Sciences (NTZ), Universität Leipzig,
Postfach 100 920, D-04009 Leipzig, Germany*

Michael Bachmann[‡]

*Center for Simulational Physics, The University of Georgia, Athens, Georgia 30602, USA; Instituto de Física,
Universidade Federal de Mato Grosso, 78060-900 Cuiabá, Mato Grosso, Brazil; and Departamento de Física,
Universidade Federal de Minas Gerais, 31270-901 Belo Horizonte, Minas Gerais, Brazil*

We construct the complete structural phase diagram of polymer adsorption at substrates with attractive stripelike patterns in the parameter space spanned by the adsorption affinity of the stripes and temperature. Results were obtained by extensive generalized-ensemble Monte Carlo simulations of a generic model for the hybrid organic-inorganic system. By comparing with adhesion properties at homogeneous substrates, we find substantial differences in the formation of adsorbed polymer structures if translational invariance at the surface is broken by a regular pattern. Beside a more specific understanding of polymer adsorption processes, our results are potentially relevant for the design of macromolecular pattern recognition devices such as sensors.

Interfacial macromolecular recognition is essential and ubiquitous in biology processes and of potential interest for nanotechnological applications. For these reasons, a thorough understanding of the generic features that promote the adsorption of polymers at attractive substrates under the influence of thermal fluctuations is of undeniable relevance. The complex interplay of generic, undirected environmental effects (as, e.g., controlled by the temperature) and system-specific parameters that enable the formation of stable, ordered structural phases of the polymer near the substrate requires systematic research.

Consequently, the statistical mechanics of adsorption transitions of entire classes of such hybrid systems can be investigated only by means of efficient stochastic Monte Carlo computer simulations. Computational studies have already been done extensively in the past for the adsorption of lattice polymers and proteins [1–8] and off-lattice polymer models [9–11] at homogeneous, flat substrates. Various other geometries of substrates have been investigated as well, such as polymer adsorption under confinement in spherical cavities [12], at cylindrical [13,14] and fluctuating membranelike surfaces [15], and at nanowires [16,17]. The recognition of substrates and surface patterns by polymers and proteins has also been the subject of numerous experimental and computational studies [18–24]. What is still lacking, but essential for the turnover from empirical to systematic design of macromolecular pattern-recognizing devices, is the understanding of the change of the generic structural behavior of macromolecules in the vicinity of an attractive substrate if the homogeneous surface is replaced by a patterned interface.

In this Letter, we compare the structural phase diagrams of molecular adsorption at homogeneous and heterogeneous substrates for entire classes of substrates that are characterized by their adsorption propensity. We will unravel the complex structure formation processes and the stable structural phases that are formed by competing energetic interactions such as surface attraction strength and intramolecular forces and also entropic effects due to thermal activation and the repercussions of finite-size effects.

For our study, we introduce a generic model for the adsorption of a self-interacting polymer at a complex surface with a stripe pattern. It is sufficiently simple to enable a comprising computational study of all structural phases of the hybrid system, but it is also specific enough to identify the differences between polymer adsorption behavior at homogeneous and patterned substrates.

The polymer is modeled by a linear bead-stick model with stiff bonds of length unity. Nonbonded intramolecular interactions are described by a standard Lennard-Jones potential; the sum over all pairwise contributions reads

$$E_{\mathrm{LJ}}/\varepsilon = 4 \sum_{i=1}^{N-2} \sum_{j=i+2}^{N} \left[\left(\frac{\sigma}{r_{ij}} \right)^{12} - \left(\frac{\sigma}{r_{ij}} \right)^{6} \right], \qquad (1)$$

where r_{ij} is the distance between two nonbonded monomers i and j; $N = 40$ is the number of monomers in the polymer chain. In our model, the intramolecular interaction sets the overall energy scale ε, in which also all other energies will be measured. The length scale of this

interaction (van der Waals diameter) matches that of the bond length $r_{ii+1} \equiv b$: $\sigma/b = 1$, which will serve as the basic unit for all other lengths as well. As a reference to DNA/RNA and protein systems, an effective overall stiffness of the chain is introduced by the bending energy $E_{bend}/\varepsilon = \epsilon_{bend} \sum_{i=1}^{N-2}(1 - \cos\vartheta_i)$, where ϑ_i is the bending angle between monomers i, $i+1$, and $i+2$ and $\epsilon_{bend} = 1/4$.

The surface of the substrate is located at $z = 0$ and possesses a periodic stripe pattern that is oriented in the y direction. The bulk of the substrate ($z < 0$) is homogeneous. The interaction of the polymer chain with the patterned substrate is described by [9,11]

$$E_s/\varepsilon = \sum_{i=1}^{N} \epsilon_{sub}(x_i) \left[\frac{2}{15} \left(\frac{\sigma_s}{z_i} \right)^9 - \left(\frac{\sigma_s}{z_i} \right)^3 \right] \qquad (z_i > 0),$$

(2)

where the same length scale as above has been chosen ($\sigma_s/b = 1$). The 9-3 Lennard-Jones–like potential follows by integrating a 12-6 Lennard-Jones potential over the half-space $z < 0$. We quantify the effect of the stripe pattern by the periodic x-dependent dimensionless adsorption strength parameter

$$\epsilon_{sub}(x) = \epsilon_s + \epsilon_{stripe} \begin{cases} \cos^2[\alpha(x)\pi], & \text{if } |\alpha(x)| \leq 1/2, \\ 0, & \text{otherwise,} \end{cases}$$

(3)

where the choice $\alpha(x) = [(x/\sigma_x + 1/2) \mod D] - 1/2$ [25] guarantees that the periodic potential is maximally

attractive at the stripe locations $x_{max}^{(k)} = \pm kD\sigma_x$ (k integer), smoothly decays towards $x_{max}^{(k)} \pm \sigma_x/2$, and is zero otherwise. As for all other length scales, we set $\sigma_x/b = 1$ in the simulations. The distance between the stripes was chosen to be $D = 5$.

Thus, the total energy of any polymer conformation is given by $E = E_{LJ} + E_{bend} + E_s$. The hybrid model and the effective surface potential strength that is felt by each monomer are depicted in Fig. 1. To prevent the nongrafted polymer from escaping, a steric wall is placed at $z = 60$. The influence of this constraint upon the translational entropy is well understood [11]. There are no boundaries in the x and y directions.

With this model, the two cases of substrate types, homogeneous and patterned, can be compared systematically. Homogeneous substrates are represented by $\epsilon_{stripe} = 0$, and the only energy scale associated with the surface potential that competes with the polymer parameters is governed by ϵ_s. This case has been investigated in detail in Refs. [9,11]. The hyperphase diagram for a
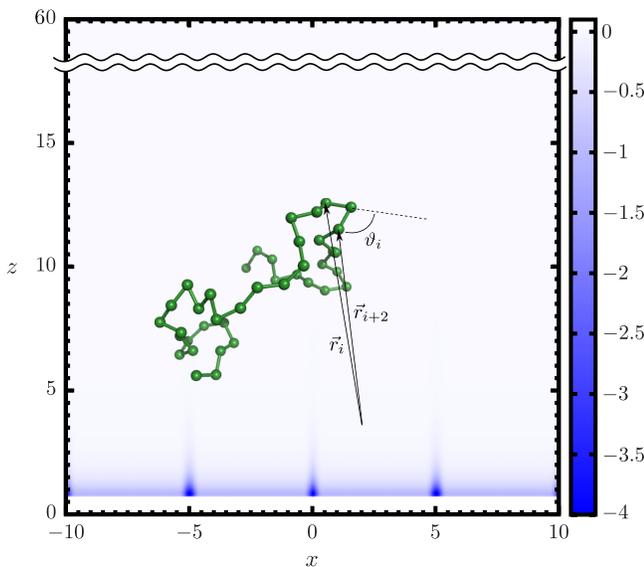

FIG. 1 (color online).   Polymer near a substrate with a stripe pattern; the surface is located at $z = 0$. The density plot represents the periodic surface potential. The steric wall at $z = 60$ regularizes the translational entropy in the half-space $z > 0$.
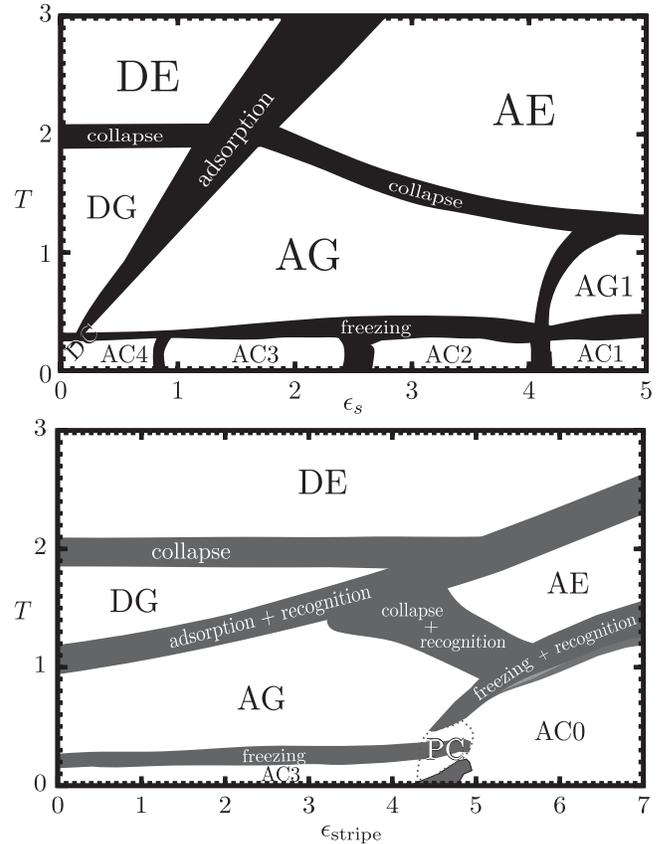

FIG. 2.   Hyperphase diagrams of structural polymer phases for homogeneous substrates (top) with $\epsilon_{stripe} = 0$ and for substrates with the stripe pattern (bottom), where $\epsilon_s = 1$. In A (D) phases, polymer structures are preferably adsorbed (desorbed). The second letter indicates increasing order in these phase regions: expanded (E), globular (G), and compact (C); PC is short for "phase coexistence." Temperatures T are given in units of ε/k_B.

40-mer, parametrized by ϵ_s and temperature T, is shown in Fig. 2(top). The more interesting case of the patterned substrate is simulated by adjusting the homogeneous component of the surface energy by setting $\epsilon_s = 1$ and by considering ϵ_{stripe} as a variable parameter.

We simulated this system at 71 fixed values of ϵ_{stripe} with the parallel tempering Monte Carlo method [26], using in each case 72 replicas at different temperatures. The total number of sweeps amounted to 10^{10}.

The structural hyperphase diagram that corresponds to this case is shown in Fig. 2(bottom), also for a polymer with $N = 40$ monomers. This is the central result of our study. The monotonic behaviors of various canonical response quantities, such as the specific heat and fluctuations of structural quantities (gyration tensor components and contact numbers), were investigated and regions of thermal activity identified (peaks and "shoulders"). The accumulation of these signals is represented by the transition bands shown in the phase diagrams. Since the system is finite, the width of the bands is a systematic uncertainty [9]. As usual, it should be noted that (pseudo)transitions between structural phases shall not be confused with thermodynamic phase transitions, although the origin of the structural transitions, cooperativity, is similar. In exemplary simulations of longer chains with up to 80 monomers, we do not observe qualitative changes in the phase behavior; i.e., the results for $N = 40$ are representative.

Before discussing the novel features of adsorption behavior under the influence of the pattern potential, let us review the main structural phases of the homogeneous case first, as shown in Fig. 2(top). The adsorption transition line separates the major adsorbed phases of expanded (random-coil) structures (AE), globular adsorbats (AG), and compact, crystalline structures (AC) from the well-known desorbed phases of expanded (DE), globular (DG), and compact conformations (DC). Particularly noteworthy are the topological transitions from three-dimensional conformations to two-dimensional films ($AE \rightarrow AG1$ and $AG \rightarrow AG1$), as well as the layering transitions towards ACn, where n denotes the number of layers in the conformation [9,11]. By comparing the results for various system sizes and also with lattice results, no obvious indications could be found that the general phase structure will substantially change towards the thermodynamic limit. Even the hierarchical solid-solid (layering) transitions from mono- to multiple-layer phases are surprisingly persistent. Representative polymer conformations are shown for all phases in Fig. 3.

The structural phase diagram for polymer adsorption at a striped substrate, as shown in Fig. 2(bottom), is also generic in large parts, but it depends on the overall attraction strength of the substrate (in our model ϵ_s). We chose $\epsilon_s = 1$, because in this case the energy scale of the overall attraction strength of the substrate is identical to the nonbonded intramolecular energy scale. This has the
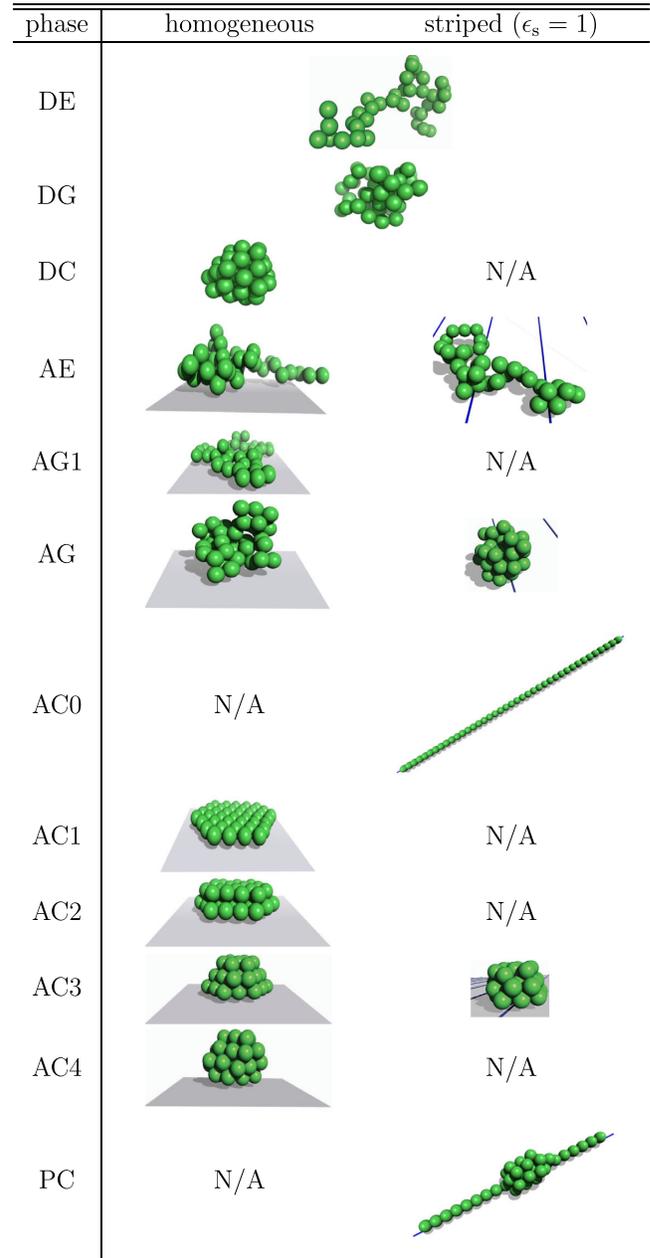

phase	homogeneous	striped ($\epsilon_s = 1$)
DE		
DG		
DC		N/A
AE		
AG1		N/A
AG		
AC0	N/A	
AC1		N/A
AC2		N/A
AC3		
AC4		N/A
PC	N/A	

FIG. 3 (color online). Examples of typical conformations in the different structural phases for homogeneous ($\epsilon_{stripe} = 0$) and striped substrates (with $\epsilon_s = 1$).

advantage that the limit $\epsilon_{stripe} = 0$ is nontrivial (standard adsorption at a homogeneous substrate) and the phase structure in the chosen temperature interval is balanced; i.e., there are distinct desorbed and adsorbed phases. Thus, the cross sections at $\epsilon_{stripe} = 0$ in the phase diagram in Fig. 2(bottom) and at $\epsilon_s = 1$ in Fig. 2(top) are identical, which is why in the desorbed region only DG and DE are present, but not DC. The most compact polymer structures are those with three layers ($AC3$). The adsorption transition line separates the globular regimes DG and AG. The general phase structure and thus also the dominant polymer

conformations are virtually the same for both classes of substrates. It should be noted that the correspondence between both substrate classes holds also for other values of ϵ_s, as long as ϵ_{stripe} does not exceed a specific threshold value (here it is $\epsilon_{\text{stripe}} \approx 3$, where phase AE starts mixing in).

Regarding the polymer structures, the essential difference between the adsorption processes on both types of substrates is that the polymer prefers the contact to the energetically more favorable stripe regions on the patterned substrate. Since the extension (radius of gyration in the xy plane) of the compact conformations in AG and $AC3$ is smaller than the distance between the stripes, the polymer recognizes exactly one stripe upon adsorption. We here generally consider an adsorption transition to be a recognition process if the polymer adjusts to the surface pattern in any form. In this case, the space between the stripes is virtually emptied; i.e., the $AG/AC3$ phases in the case of the patterned substrate have a different appearance than their analogs in the homogeneous case. Effectively, the presence of the stripes reduces the translational entropy on the substrate. For the same reason, the adsorption from DG to AG is a docking process with no apparent refolding. The increased attraction affinity of the patterned substrate caused by the stripes leads to an increased adsorption temperature. The freezing transition from AG to $AC3$ remains virtually unaffected by an increase of ϵ_{stripe} in this region ($\epsilon_{\text{stripe}} < 4.5$): Once the polymer has docked in phase AG, it only reorders monomers upon further cooling to optimize the number of internal contacts and the distance of each monomer to the stripe it binds to.

In phase DE, entropy clearly dominates over nonbonded polymer energy and conformations are unstructured. Lowering the temperature leads to adsorption but not ordering; i.e., the adsorption phase AE forms. The energetic attraction of the stripes is larger than the homogeneous regions of the substrate, so the polymer recognizes the existence of the stripes, but its typical extension is larger than the distance between two stripes. Therefore, the polymer structures attach to several stripes simultaneously but in no specific way. For comparatively large stripe attraction strength ($\epsilon_{\text{stripe}} > 6$), the polymer undergoes a direct transition from AE to a singular regime that has no relevance on homogeneous substrates. This is the "rodlike" phase $AC0$ of linelike structures, where all monomers prefer contact with a single stripe (see Fig. 3).

It is a truly essential feature of stripe-patterned adsorption that with $AC0$ we have identified another topological phase. Remember that the 40-mer has four AC phases on homogeneous substrates, of which $AC1$ is filmlike, i.e., two-dimensional, whereas polymer structures in $AC2$, $AC3$, and $AC4$ form the three-dimensional topological class of compact phases, where structures extend into the third dimension perpendicular to the substrate. However, $AC0$ is apparently one-dimensional.

Topological transitions between these phases are supposed to be particularly strong and persistent in the thermodynamic limit [3,4,9,11].

Another remarkable feature is the transition from $AC0$ to $AC3$ by passing a transition regime that we denote by PC (phase coexistence). Given the fact that we have chosen thin stripes with orientational interaction directed almost entirely into the direction perpendicular to the substrate, lamellar or filmlike double-rod structures (which would make up a phase $AC1$) and double-layer or triple-rod structures (that would form a phase $AC2$) have to compete with "pearl-necklace" structures as shown in Fig. 3. The result is the mixed phase PC, where the mentioned geometries coexist, but none dominates. Mixed solid phases occur for finite polymers also in DC [27].

In summary, we have identified the complete phase structure of polymers adsorbing at a substrate with a stripe pattern by means of parallel tempering Monte Carlo simulations. By comparison with known results obtained for homogeneous substrates, we found substantial differences in the adsorption behavior, where the attractive interaction of the stripes governs the formation of polymer structures at the adsorbent. We also found that a directional stripe potential favors the formation of crystalline droplets and rodlike strings at a single stripe. Consequently, the adsorption transition in the globular regime ($DE \rightarrow AE$) and the collapse or reordering transitions at the substrate ($AE \rightarrow AG$; AG, $AE \rightarrow AC0$) were identified as the only transitions, where the polymer recognizes the stripe pattern. In conclusion, our general results contribute to the systematic understanding of polymer adsorption and recognition at patterned complex surfaces, which is relevant for nonempirical approaches to the design of nanosensoric applications.

[*]Monika.Moeddel@itp.uni-leipzig.de
[†]Wolfhard.Janke@itp.uni-leipzig.de;
http://www.physik.uni-leipzig.de/CQT.html
[‡]bachmann@smsyslab.org; http://www.smsyslab.org

[1] T. Vrbová and S. G. Whittington, J. Phys. A **29**, 6253 (1996).
[2] Y. Singh, D. Giri, and S. Kumar, J. Phys. A **34**, L67 (2001); R. Rajesh, D. Dhar, D. Giri, S. Kumar, and Y. Singh, Phys. Rev. E **65**, 056124 (2002).

[3] M. Bachmann and W. Janke, Phys. Rev. Lett. **95**, 058102 (2005); Phys. Rev. E **73**, 041802 (2006).

[4] J. Krawczyk, A. L. Owczarek, T. Prellberg, and A. Rechnitzer, Europhys. Lett. **70**, 726 (2005).

[5] M. Bachmann and W. Janke, Phys. Rev. E **73**, 020901(R) (2006).

[6] J. Luettmer-Strathmann, F. Rampf, W. Paul and K. Binder, J. Chem. Phys. **128**, 064903 (2008).

[7] A. D. Swetnam and M. P. Allen, Phys. Chem. Chem. Phys. **11**, 2046 (2009).

[8] Y. W. Li, T. Wüst, and D. P. Landau, Phys. Rev. E **87**, 012706 (2013).

[9] M. Möddel, M. Bachmann, and W. Janke, J. Phys. Chem. B **113**, 3314 (2009).

[10] L. Wang, T. Chen, X. Lin, Y. Liu, and H. Liang, J. Chem. Phys. **131**, 244902 (2009).

[11] M. Möddel, W. Janke, and M. Bachmann, Phys. Chem. Chem. Phys. **12**, 11548 (2010); Macromolecules **44**, 9013 (2011).

[12] H. Arkın and W. Janke, Phys. Rev. E **85**, 051802 (2012); J. Phys. Chem. B **116**, 10379 (2012); J. Chem. Phys. **138**, 054904 (2013); Eur. Phys. J. Spec. Top. **216**, 181 (2013).

[13] A. Milchev and K. Binder, J. Chem. Phys. **114**, 8610 (2001).

[14] I. Gurevitch and S. Srebnik, Chem. Phys. Lett. **444**, 96 (2007); J. Chem. Phys. **128**, 144901 (2008).

[15] S. Karalus, W. Janke, and M. Bachmann, Phys. Rev. E **84**, 031803 (2011).

[16] T. Vogel and M. Bachmann, Phys. Rev. Lett. **104**, 198302 (2010).

[17] T. Vogel, T. Mutat, J. Adler, and M. Bachmann, Commun. Comput. Phys. **13**, 1245 (2013).

[18] N. Gupta and A. Irbäck, J. Chem. Phys. **120**, 3983 (2004).

[19] T. Bogner, A. Degenhard, and F. Schmid, Phys. Rev. Lett. **93**, 268108 (2004).

[20] J. J. Cerdà and T. Sintes, Biophys. Chem. **115**, 277 (2005).

[21] Y. A. Kriksin, P. G. Khalatur, and A. R. Khokhlov, J. Chem. Phys. **122**, 114703 (2005).

[22] K. Sumithra and E. Straube, J. Chem. Phys. **125**, 154701 (2006).

[23] M. Bachmann, K. Goede, A. G. Beck-Sickinger, M. Grundmann, A. Irbäck, and W. Janke, Angew. Chem., Int. Ed. **49**, 9530 (2010).

[24] A. D. Swetnam and M. P. Allen, Phys. Rev. E **85**, 062901 (2012).

[25] The modulo operation $v \bmod w$, where v and w are real numbers, is given by the floor function: $v \bmod w = v - w \lfloor \frac{v}{w} \rfloor$, where $\lfloor a \rfloor$ is the largest integer not greater than a.

[26] K. Hukushima and K. Nemoto, J. Phys. Soc. Jpn. **65**, 1604 (1996).

[27] J. Gross, T. Neuhaus, T. Vogel, and M. Bachmann, J. Chem. Phys. **138**, 074905 (2013).